Pure & Appl. Chem., Vol. 62, No. 8, pp. 1511–1520, 1990.
Printed in Great Britain.

A chemical approach toward photosynthetic reaction center

Kazuhiro Maruyama* and Atsuhiro Osuka

Department of Chemistry, Faculty of Science, Kyoto University, Kyoto 606, Japan

Abstract—A series of conformationally restricted dimeric porphyrins bridged by aromatic spacers has been synthesized. Soret bands of their bis-zinc complexes are split due to the exciton coupling, depending upon the geometrical relationship of the two porphyrin rings. With these dimeric porphyrins, the geometry-dependence of the intramolecular singlet excitation energy transfer (EN) in the zinc-free base diporphyrin system and the intramolecular electron transfer (ET) in the zinc-ferric hybrid diporphyrin system were studied by the pico-second time-resolved fluorescence spectroscopy and pico-second time-resolved transient absorption spectroscopy. It has been shown that the former process proceeds via Förster mechanism. In the latter system, both rates of the forward and backward ET were determined. The rates of the forward ET decreased upon the increase of the center-to-center distance of the two porphyrins, while the rates of the backward ET were nearly constant through the series in the range of 8-22 Å of the center-to-center distance. An improved procedure has been developed for the synthesis of conformationally restricted trimeric and pentameric porphyrins as well as quinone-linked porphyrin aggregates, which will be very useful in studying the sequential and long-distance EN and ET processes.

1. INTRODUCTION

It has now been six years since the publication of the crystal structure of the photosynthetic reaction center of the purple bacterium Rhodopseudomanas viridis (ref. 1). From this and the subsequent works on Rhodobacter sphaeroides (ref. 2), we have a reasonably precise knowledge of the location of the chromophores involved in photosynthetic charge separation, as well as the surrounding protein environment. Nevertheless, the remarkable features of the primary charge separation (ultrafast, ca. 3 ps, electron transfer through long distance, 17 Å, much slower recombination compared to forward electron transfer), have yet to be definitely accounted for. Characterization of these natural systems has been aided by the synthesis of a variety of artificial models such as covalently-linked porphyrin dimers and quinone-linked porphyrins (ref. 3). In a program aimed at the development of artificial photocatalyst capable of efficient charge separation, we are attempting to understand the geometry-dependence of excitation energy transfer (EN) and electron transfer (ET) processes on the basis of synthetic model compounds. Synthetic models with well-defined distances and mutual orientations are particularly effective in probing this problem.

2. SYNTHESIS AND OPTICAL PROPERTIES OF CONFORMATIONALLY RESTRICTED DIMERIC PORPHYRINS

We have synthesized a series of conformationally restricted dimeric porphyrins bridged by aromatic spacers (Fig. 1)(ref. 4 and 5). In these dimeric porphyrins, two porphyrin rings are rigidly held in a certain geometry by the combined steric restrictions of the spacer and the flanking ethyl groups.

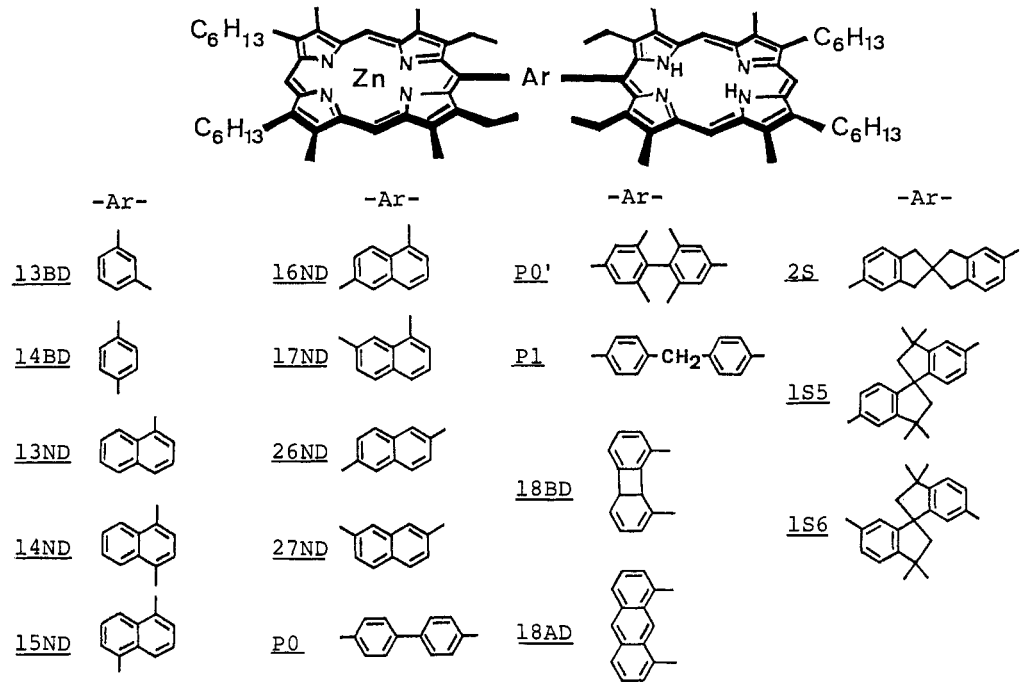

Fig. 1. Structures of conformationally restricted dimeric porphyrins. M1=M2=Zn; bis-zinc complexes. M1=Zn and M2=H2; mono-zinc complexes. M1=Zn and M2=Fe(III)Cl; zinc-ferric hybrid complexes.

Consequently, the aromatic bridge remains perpendicular to the mean porphyrin plane, thereby minimizing direct π-π interaction between the porphyrin and the bridge. Spiro-biindane spacers were employed with aims at mimicking the twisted orientations of chromophores such as hemes and chlorophylls in natural systems (2S and 1S5) and at mimicking the twisted partially overlapping geometry of the special pair in bacterial photosynthetic reaction center (1S6). All these dimeric porphyrins were synthesized from the corresponding aryl dialdehydes by the method of Chang (ref. 6).

In Fig. 2, the absorption spectra of 1N(Zn) and the bis-zinc complexes of the naphthalene-bridged dimeric porphyrins ND(Zn2) in dichloromethane are presented. All bis-zinc complexes of ND(Zn2) showed split Soret bands. Interestingly, as the dihedral angle of the two porphyrins decreases from a flat dimer 26ND(Zn2) to a stacked dimer 17ND(Zn2), the relative intensity at the longer wavelength decreases and instead the relative intensity at the shorter wavelength increases. And finally a face-to-face dimer 18BD(Zn2) displays a completely blue-shifted Soret band at 388 nm. These systematic spectral changes are qualitatively in accordance with the simple selection rule (ref. 7) predicted from the theory of exciton coupling, which has often

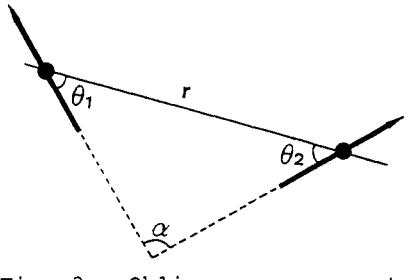

Fig. 3. Oblique arrangement of two transition dipole moments.

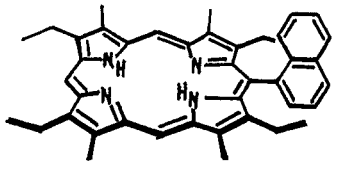

1N

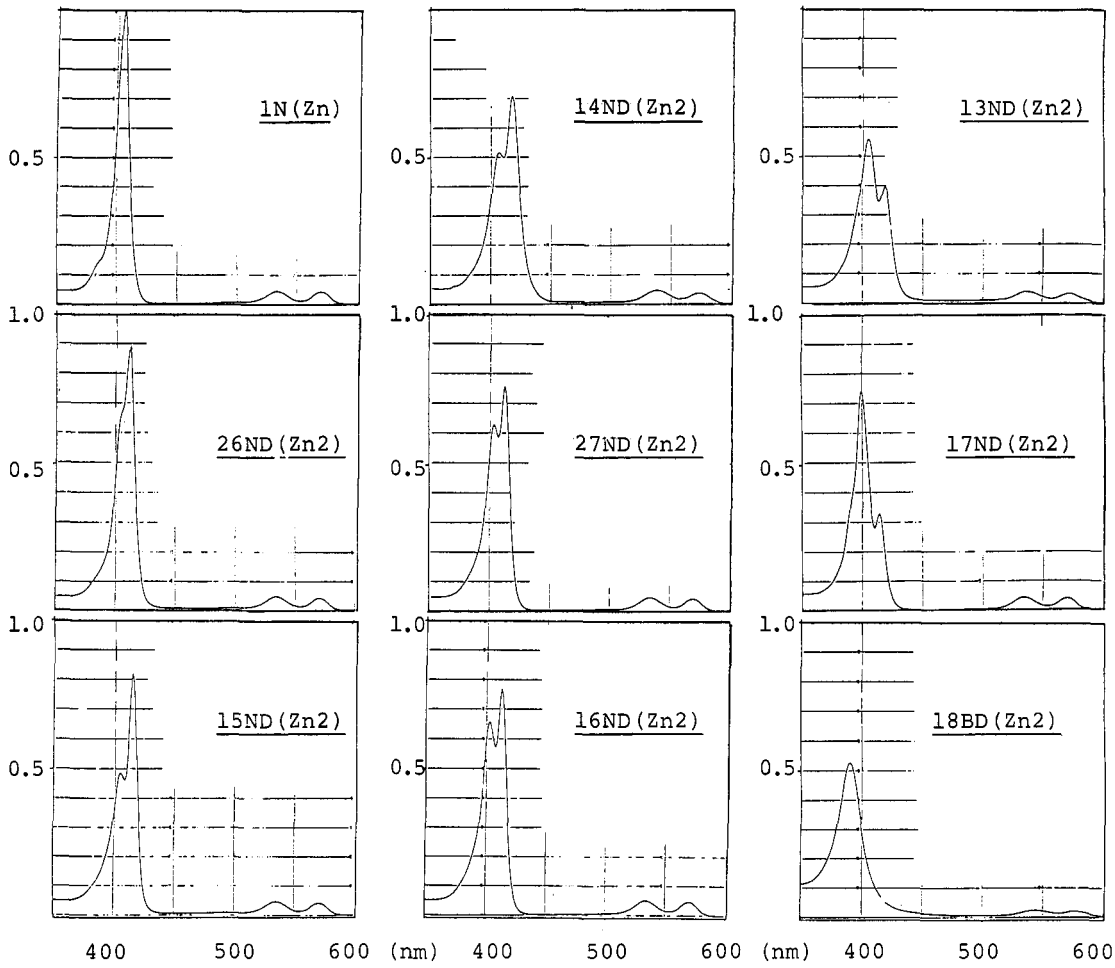

Fig. 2. Absorption spectra of 1N(Zn) and ND(Zn2) in dichloromethane. Concentrations were 2.0×10^{-6} M for 1N(Zn) and 1.0×10^{-6} M for ND(Zn2).

been used to explain the unusual electronic spectral properties of non-covalent porphyrin aggregates and covalently-linked porphyrin dimers. However, to the best of our knowledge, there exists no reliable and systematic synthetic model for certification of the theory in fluid solution containing porphyrins, particularly on the dependence of coupling energy upon the geometrical parameters. According to the theory, the dipole-dipole exciton splitting energy, ΔE, in the oblique geometry as shown in Fig. 3, is given by eq. (1);

$$\Delta E = 2|M|^2 (\cos \alpha + 3\cos \theta_1 \cos \theta_2)/r^3 \qquad (1)$$

where $|M|$ is the transition dipole moment of the monomer. A plot of ΔE vs. the geometrical parameter, $2(\cos \alpha + 3\cos\theta 1 \cos\theta 2/)r^3)$, showed a good linear correlation between these two quantities. From the slope, the magnitude of the transition dipole moment of the monomer $|M|$ effective for the exciton coupling was determined to be 7.9 D. This is in good agreement with the value (9.7 D) of the transition dipole moment of the monomer 1N(Zn) calculated from its absorption spectrum.

The fluorescence properties of ND(Zn2) were virtually identical with that of 1N(Zn), indicating the absence of significant perturbation in their S1 states in contrast to the strong exciton coupling of their S_2 states. The fluorescence quantum yield of 18AD(Zn2) was about one-third those of 1N(Zn), and

18BD(Zn2) was nearly non-fluorescent. These observations indicated the maximal exciton interaction in the face-to-face-geometry, which resulted in the significant perturbation even in their S_1-states.

3. GEOMETRY-DEPENDENCE OF INTRAMOLECULAR EXCITATION ENERGY TRANSFER REACTION AND ELECTRON TRANSFER REACTION

Restricted conformations of these models are particularly useful in relating kinetic data with the geometrical factors such as distance and orientation. Therefore, we have studied the geometry-dependence of the intramolecular excitation energy transfer (EN) reaction in the mono zinc complexes ZnP-H2P (ref. 8), and of the intramolecular electron transfer (ET) reaction in the ZnP-ferric porphyrin chloride hybrid complexes ZnP-Fe(III)ClP (ref. 9).

3.1 Intramolecular excitation energy transfer (EN) in ZnP-H2P

In the steady-state fluorescence spectra of ZnP-H2P, the fluorescence intensity of the ZnP decreased significantly (λem 577 and 628 nm) whereas that of the H2P was strongly enhanced (λem 628 and 693 nm), showing that efficient singlet excitation energy transfer occurred from the ZnP to the H2P. This was confirmed by the picosecond time-resolved fluorescence spectra. For example, the time-resolved fluorescence spectra of 27N(Zn-H2) taken by excitation at 570 nm in dichloromethane are shown in Fig. 4. The fluorescence spectrum at 10 ps was assigned primarily due to the ZnP. The decay of the ZnP fluorescence was followed by the rise of the H2P fluorescence. The rate of intramolecular EN, k(e), was determined by measuring fluorescence decay (λ em 580 nm) of the ZnP. Importantly, most of the diporphyrins exhibited virtually a single decaying component, indicating that the singlet excited state of the ZnP is quenched by the H2P through a single conformation.

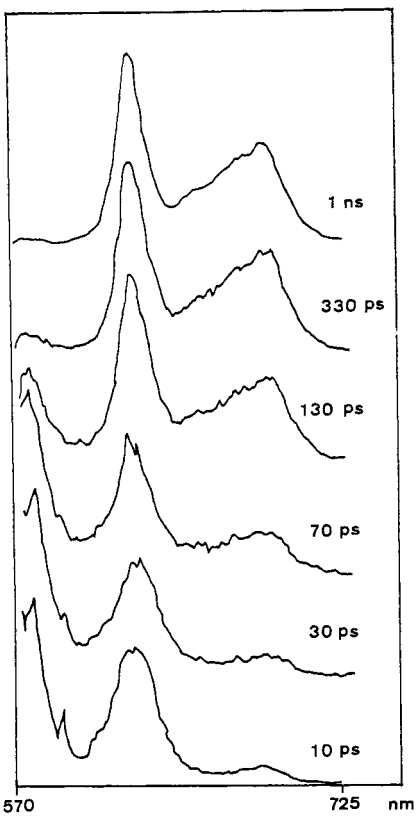

Fig. 4. Time-resolved fluorescence spectra of 27ND(Zn-H2) in dichloromethane. The excitation wavelength is 570 nm.

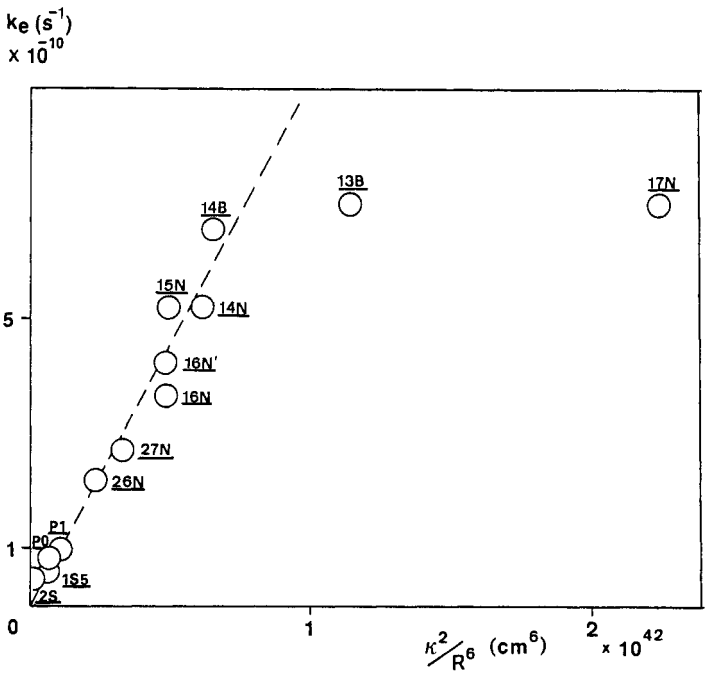

Fig. 5. A plot of the rate of singlet excitation energy transfer (ke) vs. the geometrical parameter, (K^2/r^6). Since the calculated value for 18AD(Zn-H2) is ca. 4.0×10^{43} cm^{-6}, its plot is omitted from this figure.

The fluorescence properties of the ZnP-H2P hybrid diporphyrins have been well documented (ref. 10). There is considerable overlap between the fluorescence emitted by the ZnP and the ground-state absorption spectrum of the H2P, indicating that EN should be extremely efficient. In the Forster mechanism, the rate of singlet EN can be expressed in terms of the orientation factor (K) and the center-to-center distance (r) between the transition dipole moments;

$$k(e) = \frac{9000\,(\ln 10)\,K^2\,\phi f}{128\,\pi^5\,n^4\,N\,R^6} \int \frac{fs(\upsilon)\,Ea(\upsilon)}{\upsilon^4}\,d\upsilon \quad (2)$$

where n is the refractive index of the solvent, N is Avogadoro's number, ϕf is the fluorescence quantum yields (0.04) of the donor, υ is the wave number, $Ea(\upsilon)$ is the molar extinction coefficient of the acceptor and $fs(\upsilon)$ is the spectral distribution of fluorescence normalized such that $fs(\upsilon)d = 1$. Evaluation of the overlap integral Ω gives a value of 3.5×10^{-11} $cm^6\ mol^{-1}$, which is reasonable agreement with the value of 5.0×10^{-11} $cm^6\ mol^{-1}$ given by Brookfield (ref. 10). The orientation factor (K) is written by eq. (3);

$$K = \cos\theta - 3\cos\theta 1\ \cos\theta 2 \quad (3)$$

where θ being the angle between the transition dipoles; $\theta 1$, $\theta 2$ are the angles between the dipoles and the radius vector adjoining them. For diporphyrins linked by flexible methylene chains, K^2 is usually regarded 2/3 by assuming complete random geometries. In our conformationally constrained diporphyrins, it is possible to estimate both r and K. As shown in Fig. 5, a plot of k(e) vs the geometrical parameter (K^2/r^6) showed a good linear correlation between these two quantities. Significant deviation of 18AD(Zn-H2), 13BD(Zn-H2), and 17ND(Zn-H2) from the plot may indicate the limitation of the theory based on the point-dipole approximation at small distance r. The experimentally observed slope in Fig. 5 is 0.9×10^{-31} $cm^6\ s^{-1}$, which is roughly in a same magnitude with the calculated value of 2×10^{-31} $cm^6\ s^{-1}$, indicating the excitation energy transfer by Forster mechanism.

3.2 Intramolecular electron transfer (ET) in ZnP-Fe(III)PCl

Covalently-linked electron donor-acceptor molecules have been extensively studied in order to gain information about the factors governing the intramolecular electron transfer (ET) reactions (ref. 3). One of the most important requirements for these molecules to be an efficient photocatalyst for charge separation is that the molecule is organized so as to allow very fast photoinduced ET and to make the thermal wasteful backward ET much slower than the forward ET. Such a molecular organization is actually realized in the bacterial photosynthetic reaction center.

The fluorescence spectra of the ZnP-Fe(III)PCl are that of the unperturbed ZnP alone but their fluorescence quantum yields decrease dramatically. This decrease in the fluorescence quantum yields can be ascribed to the intramolecular ET (charge separation) from the singlet excited state of the ZnP to the Fe(III)P on the basis of the picosecond transient absorption measurements. As an example, the transient absorption spectra of P1(Zn-Fe) in DMF are shown in Fig. 6. The spectrum at the delay time of 26 ps was almost due to the Sn←S1 transition of the ZnP. A rapid decay of the Sn←S1 absorption at 460 nm was followed by the rise of a broad absorption in the 480-510 nm and 600-750 nm regions, which can be ascribed to the formation of $(ZnP)^+$-Fe(II)P on the basis of the previous studies (ref. 11). The time constant of the decay at 460 nm (52 ps) agreed satisfactorily with the fluorescence lifetime of the ZnP (50 ps). Upon further increase of the delay time to 3 and 5 ns, the $(ZnP)^+$-Fe(II)P decayed slowly by backward ET (charge recombination). The absorption at 450 nm which remained in the spectrum at 5 ns was assigned to the absorption spectrum due to the Tn←T1 transition of the ZnP. By analyzing a slow decay of the absorption at 510 nm, the rate constant for charge recombination, k(cr), was determined to be 6.3×10^8 s^{-1}. In a similar manner, both rate constants for charge separation and recombination were determined in a series of diporphyrin molecules. The rate constants for charge separation, k(cs),

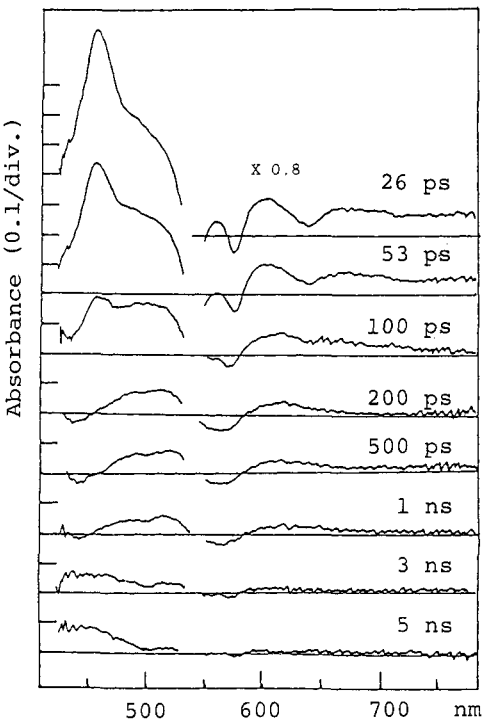

Fig. 6. Pico-second time-resolved resolved transient absorption spctra of P1(Zn-Fe) in DMF, excited at 532 nm.

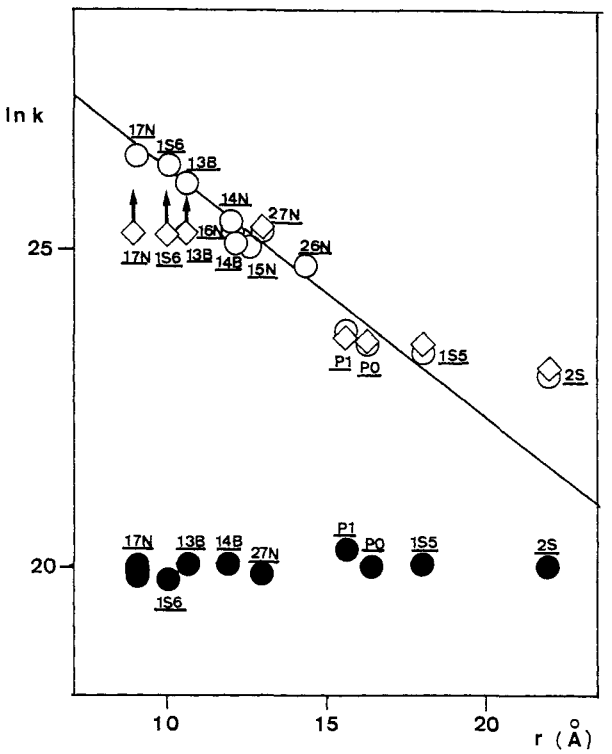

Fig. 7. Plots of lnk(cs) and lnk(cr) vs. the center-to-center distance, r; (○), k(cs) determined by the fluorescence lifetime of the ZnP; (◇), k(cs) determined by the transient absorption; (●), k(cr) determined by the transient absorption.

were more accurately determined from their respective fluorescence lifetimes, assuming that the sole additional decay route in $^{1}(ZnP)^{*}$-Fe(III)P was due entirely to the formation of $(ZnP)^{+}$-Fe(II)P. In Fig. 7, these electron transfer rate constants, k(cs) and k(cr), are plotted against the center-to-center distance between two porphyrins, r. The rate of the charge separation k(cs) decreased upon the increase of the distance r in an ordinary manner. In marked contrast, k(cr) were much smaller than k(cs) and remained nearly constant (ca. 4-6 x 10^{8} s^{-1}) through the series (in the range of 8-22 Å of r), independent of the distance, the orientation, and the structure of the intervening spacer. As a result of these effects, the increase of the ratio of k(cs)/k(cr) is brought about on decreasing the center-to-center distance. For example, the ratio of k(cs)/k(cr) increases ca. 36 times from 18 in 2S(Zn-Fe) to 650 in 1S6(Zn-Fe).

The nearly constant k(cr) values observed here might be interpreted as accidental compensation of distance effects by other factors such as orientation effects, free energy changes, or spin selection effects. Alternatively, these results suggest that the rate-determining step in the charge-recombination process is not an inter-site ET reaction but a reaction within the Fe(II)PCl complex site such as the dissociation of the Cl^{-} or the geometry change due to a shift in the position of the Fe(II) ion.

4. CONFORMATIONALLY RESTRICTED TRIMERIC AND PENTAMERIC PORPHYRIN

An improved procedure for the synthesis of conformationally restricted trimeric and pentameric porphyrin arrays has been recently developed (ref. 12). Up to data, there has been reported only one example of this type, which is the anthracene-pillared trimeric porphyrin synthesized by Chang in 1985 (ref.

13). Unfortunately, his method was found not to have general applicability and to have a defect of the scrambling of the peripheral alkyl substituents on the newly formed porphyrin ring to some extents. Our improved procedure utilized a combination of trichloroacetic acid as acid-catalyst and acetonitrile as solvent. Under these conditions, trimeric porphyrin 3 was synthesized as much as 56 % yield from 1 and 2, and a linearly-linked pentameric porphyrin 6 was synthesized from dimeric porphyrin 4 in 11 % yield, and even stacked face-to-face pentameric porphyrin 8 was constructed from the corresponding dimeric porphyrin 7 in 18 % yield. An interesting optical property accompanied by the increase of the number of the chromophore is the increase of split width observed for the Soret bands of their zinc complexes (Fig. 9). This phenomenon can also be accounted for in term of the exciton coupling theory, which predicts the exciton coupling energy in N-chromophores system should be calculated by the following eq. (4). A plot of these two quantities made a good straight line (Fig. 10), indicating the regularly repeating arrangement of the porphyrin rings in 4-6.

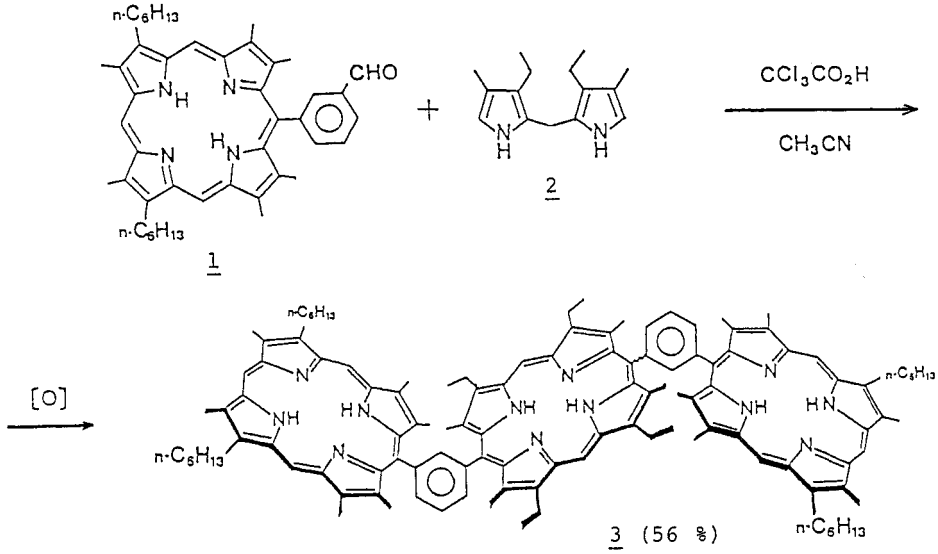

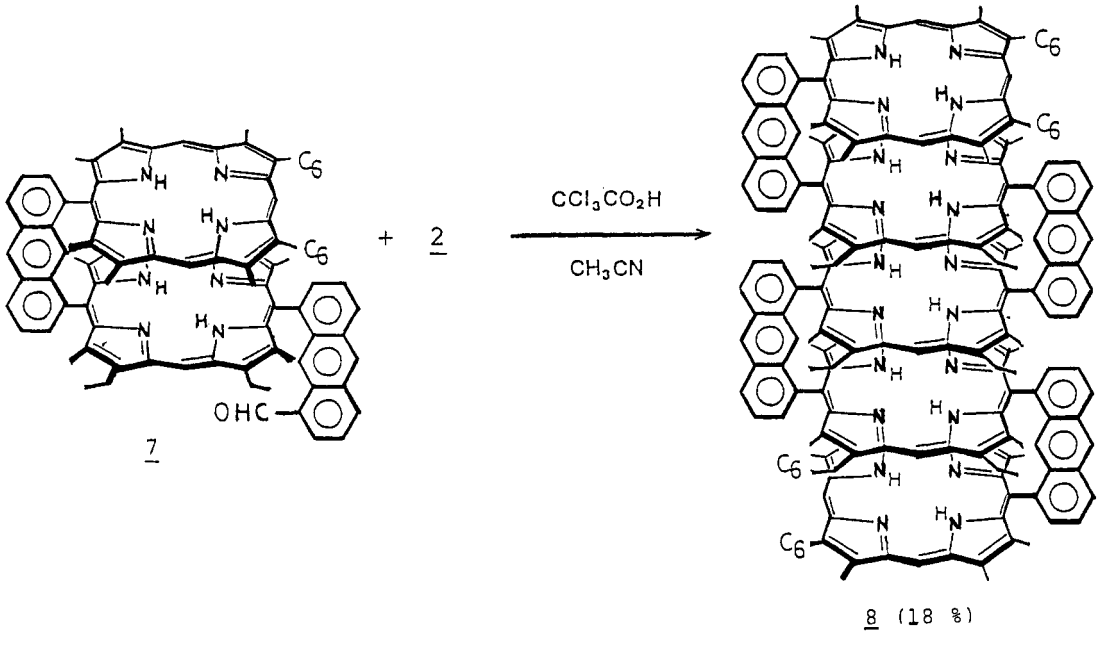

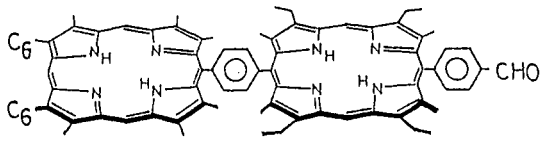

4

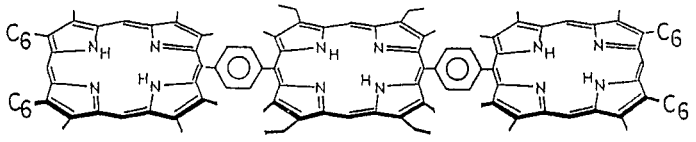

5

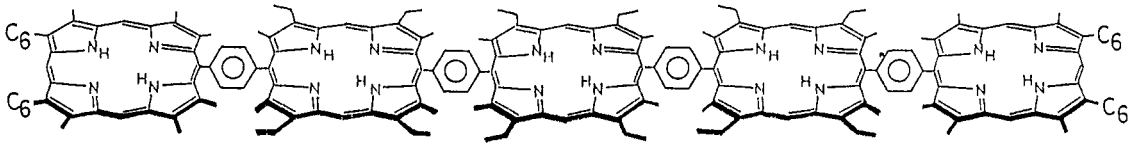

6

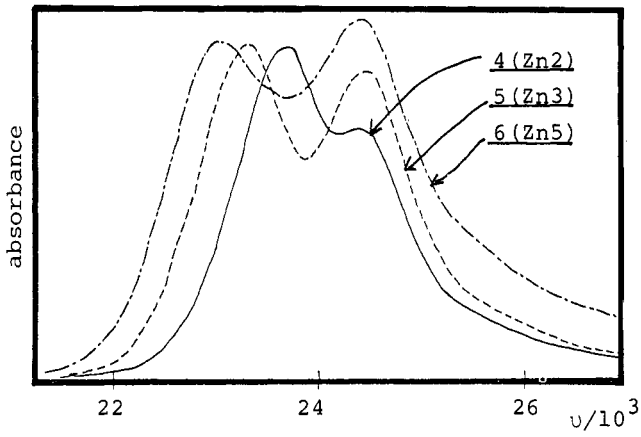

Fig. 9. The Soret absorption spectra of 4(Zn2), 5(Zn3), 6(Zn5) in 1,2-dichlorobenzene.

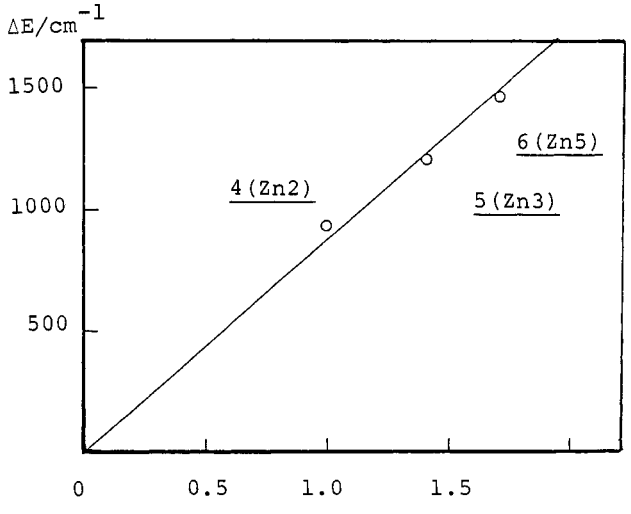

Fig. 10. A plot of exciton splitting energy ΔE vs. $2\cos(\pi/(N+1))$.

$$E = 2J\cos(\pi/(N+1)) \qquad (4)$$

Now studies aimed at mimicking sequential energy and electron transfer system based on these newly developed supramolecular compounds are under way.

5. CONFORMATIONALLY RESTRICTED QUINONE-LINKED PORPHYRINS

Porphyrins linked to quinones at restricted geometries have recently attracted considerable interest since these models allow examination of the dynamics of charge separation without concern for the conformational motions that complicate analyses of the flexible systems (ref. 14-17). In this context, porphyrin-quinone molecules 9, 10, and 11 with restricted geometries have been synthesized by our improved synthetic method (ref. 18). In these model compounds, it may be possible to investigate the outcome of sequential EN and ET reactions in conformationally restricted situations. The design of the model 11 was motivated by the attempted duplication of the whole series of L-branch of bacterial photosynthetic reaction center; strongly interacting dimers—monomer—monomer—quinone. It may be said that systematic changes of spacer and selective metallation will give a clue to understand the meanings of the complicated constitution employed by the natural photosynthetic system and will lead to the the enhancement of charge separation efficiency in an artificial system.

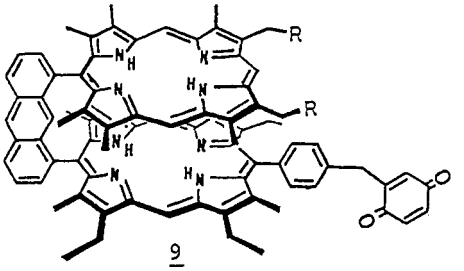

9

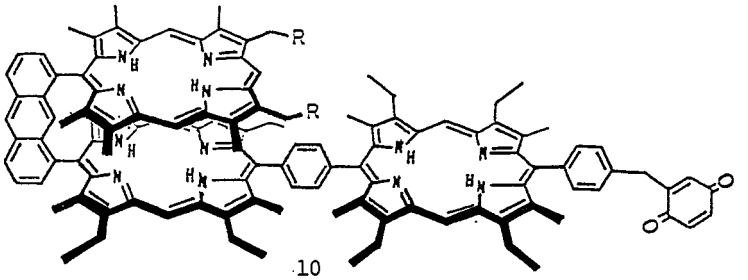

10

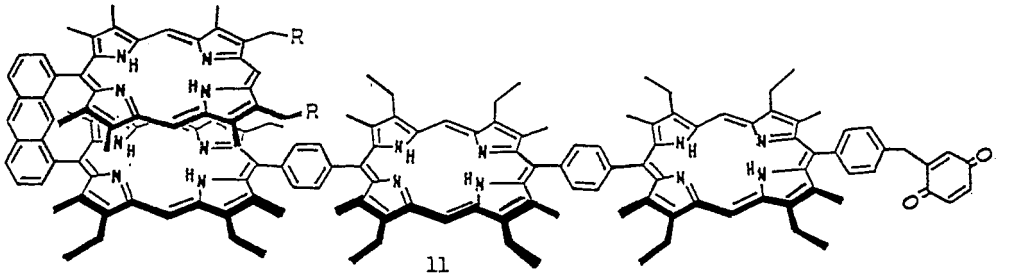

11

CONCLUSIONS

Synthetic model compounds with well-defined geometries are particularly useful in probing the geometry-dependence of important photophysical processes such as EN and ET. The chemistry described in this article is still in progress in this laboratory. We have prepared highly-organized model compounds such as 9-11.

Acknowledgement

The authors wish to express their appreciation to Professor I. Yamazaki and Dr. N. Tamai for measurement of picosecond time-resolved fluorescence lifetime, and to Professor N. Mataga and Mr. T. Asahi for measurement of picosecond time-resolved absorption spectroscopy. This work was supported by the Ministry of Education, Science, and Culture of Japan, Mitsubishi Foundation for Scientific Research, Nissan Science Foundation, and the Kurata Research Grand.

REFERENCES

1. J. Deisenhofer, O. Epp, K. Miki, R. Huber, and H. Michel, J. Mol. Biol., 180, 385-398 (1984).
2. a, J. P. Allen, G. Feher, T. O. Yates, H. Komiya, and D. C. Rees, Proc. Natl. Acad. Sci. USA, **84**, 5730-5734 (1987). b, C. -H. Chang, D. M. Tiede, J. Tang, U. Smith, J. R. Norris. and M. Schiffer, FEBS Lett., 205, 82-86 (1986).
3. M. R. Wasielewski, pp161-205, in "Photoinduced Electron Transfer", Part A, M. A. Fox, and M. Chanon eds, (1988), Elsevier, Amsterdam.
4. a, A. Osuka and K. Maruyama, Chem. Lett, 825-828 (1987). b, A. Osuka, K. Maruyama, I. Yamazaki, and N. Tamai, J. Chem. Soc., Chem. Commun., 1243-1245 (1988). c, A. Osuka, K. Ida, and K. Maruyama, Chem. Lett, 741-744 (1989). d, K. Maruyama, T. Nagata, N. Ono, and A. Osuka, Bull. Chem. Soc. Jpn., 62, 3167-3170 (1989).
5. A. Osuka and K. Maruyama, J. Am. Chem. Soc, 110, 4454-4456 (1988).
6. C. K. Chang and I. Abdalmuhdi, J. Org. Chem., 48, 538-5390 (1983).
7. M. Kasha, Radiat. Res., 20, 55-71 (1963).
8. A. Osuka, K. Maruyama, I. Yamazaki, and N. Tamai, Chem. Phys. Lett., (1990), in press.
9. A. Osuka, K. Maruyama, N. Mataga, T. Asahai, I. Yamazaki, and N. Tamai, submitted.
10. R. L. Brookfield, H. Ellul, A. Harriman, and G. Porter, J. Chem. Soc., Faraday Trans., 82, 219-233 (1986), and references cited therein.
11. a, I. Fujita, T. L. Netzel, C. K. Chang, and C.-B. Wang, Proc. Natl. Acad. Sci. USA, 79, 413-417 (1982). b, N. Mataga, H. Yao, T. Okada, Y. Kanda, and A. Harriman, Chem. Phys., 131, 473-480 (1989).
12. T. Nagata, A. Osuka, and K. Maruyama, J. Am. Chem. Soc., (1990) in press.
13. I. Abdalmuhdi and C. K. Chang, J. Org. Chem., 50, 411-413 (1985).
14. A. Osuka, H. Tomita, and K. Maruyama, Chem. Lett., 1205-1208 (1988).
15. A. Osuka, K. Ida, T. Nagata, K. Maruyama, I. Yamazaki, N. Tamai, Y. Nishimura, Chem. Lett., 2133-2136 (1989).
16. M. R. Wasielewski, M. P. Niemczyk, D. G. Johnson, W. A. Svec, and D. W. Minsek, Tetrahedron, 45, 4785-4806 (1989).
17. J. L. Sessler, M. R. Johnson, and T.-Y. Liu, Tetrahedron, 45, 4767-4784 (1989).
18. A. Osuka, T. Nagata, and K. Maruyama, unpublished work in this laboratory.